Simulating Particle Beamlines using Python

Jason Sikes
Student ID: 12182609

Advised by Dr.Tim Gorringe

August 2022

Abstract

As a quick note for the SURF Program, I originally planned on doing research on data analysis for the muon g-2 experiment. However, my research adviser and decided that the scope was perhaps too narrow for ten weeks. Therefore, he proposed a new project to me, and I decided to change my project. I passed this message along to Billie Haley, and she said this change would be fine.

In order for particle accelerators to properly store and record data from particles, the incoming beam of particles must be centered and, at times, be manipulated to redirect its direction of travel. This action of influencing particle beams can be simulated using computer programming. I have used the programming language Python to simulate these particle beams and the effects of various "magnetic lenses" on the beam's path along. This program will aid additional research by increasing the confidence in experiments using pion beams before their testing has begun. Along with simulating real particle beamlines, I have used the simulation to reach conclusions on various beamline element arrangements, applications, and relations to optical principles.

1 Introduction

In recent years, there have been increasing results from experiments that hint at lepton flavor universality violation (LFUV). A promising measurement that could provide more information on LFUV is the ratio of pion decay to positrons to pion decay to muons ($R_{e/\mu}$). However, the current experimental values of $R_{e/\mu}$ are not precise enough to arrive at any new conclusions of LFUV. This is one of the primary motivations for the upcoming PIONEER experiment taking place at the Paul Scherrer Institute (PSI). The experiment is expected to reach a result that is an order of magnitude more precise. To measure $R_{e/\mu}$, PIONEER requires a continuous beam of pions. The pion beam line that has been chosen to be used for PIONEER is the $\pi E5$ Beam Line located at PSI. This beam is theorized to be more than sufficient to produce results that will have a level of

uncertainty that meets the goals of the experiment. [1]

The programming language Python has been proven to be sufficient in handling immense calculation while maintaining accuracy in simulations. Python is the language chosen for this project to simulate particle beams. Ideally, this simulation will be used by researchers studying particle beams as a way to ensure their experimental setup will produce desirable data.

2 Establishing a Working Simulation

To begin the project, I was tasked with using Python to simulate particle motion. I was able to create the basics of the simulation by using principles of optics, dynamics, and matrix algebra. The program can currently simulate particle motion in the transverse plane. Much of the foundation of the program came from the CERN Accelerator School, but I have modified it as the project has evolved and advanced.

2.1 Optics Application

Whenever a particle with momentum is in the presence of a magnetic field, a force is applied to the particle. This force is one half of the Lorentz force and is the key idea to how physicists are able to control thousands of particles traveling at speeds close to that of light simultaneously. The type of magnetic field we are immediately interested in simulating are quadrupoles. Magnetic quadrupoles are able to "push" particles towards or away from the optical axis. An example of a particle passing through a magnetic quadrupole in Figure 1.

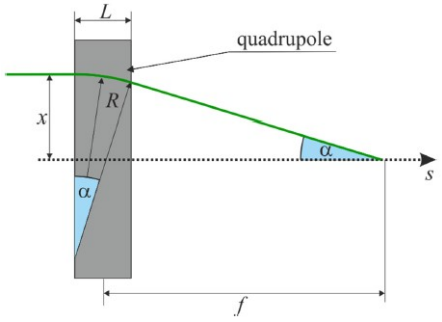

Figure 1: Example of a particle traveling through a magnetic quadrupole [2]

As seen in Figure 1, the particle exits the quadrupole region at an angle α, also called the deflection angle. Therefore, each magnetic quadrupole can be characterized by its deflection angle, and a focal length, f. This allows for an analogy to be formed between magnetic quadrupoles and thin optical lenses. Lenses also possess unique deflection angles and focal lengths. Therefore, magnetic quadrupoles can be regarded as "magnetic lenses", and optical physics can be applied to the motion of particles as if they were light.

Many of the equations from optical physics will be used to trace particle motion. Firstly, I implemented the equations for motion in the x-direction. The standard notation to describe the position of a particle is its x position (x) and it's angle relative to the optical axis (x'). There are four equations of motion to be considered here. The first two describe motion as the particle passes through a magnetic lens. Those are

$$\hat{x} = x$$
$$\hat{x'} = \frac{-x}{f} + x'$$

Here, the f is the focal length of the magnetic lens the particle traveled through. Also, it should quickly be noted that variables with a hat (ex: $\hat{x}$) indicate final positions. The second set of equations describe motion as the particle passes through space devoid of magnetic fields. These regions are also called drifts.

$$\hat{x} = x + Lx'$$
$$\hat{x'} = x'$$

Here, L is the length of the drift space. With these two final equations, the path of any particle in a beam line can be traced.

2.2 Particle Tracing in Python

The first hurdle in writing the program that simulates particle motion is the implementation of the equations. The easiest solution to this is to store the equations in matrices. Below are the matrix form of the equations for a lens and drift.

Lens
$$\begin{bmatrix} \hat{x} \\ \hat{x'} \end{bmatrix} = \begin{bmatrix} 1 & 0 \\ -\frac{1}{f} & 1 \end{bmatrix} \begin{bmatrix} x \\ x' \end{bmatrix}$$

Drift
$$\begin{bmatrix} \hat{x} \\ \hat{x'} \end{bmatrix} = \begin{bmatrix} 1 & L \\ 0 & 1 \end{bmatrix} \begin{bmatrix} x \\ x' \end{bmatrix}$$

Python makes it very easy to implement matrix multiplication and it is very quick to compute it as well. These matrices can now be used to construct fairly complicated beam lines. I will show a quick example of how Python is able to able to calculate and simplify these calculations.

I will show how to construct a simple beam line consisting of a FODO lattice. FODO is an acronym for a specific lens arrangement in which there is a focusing lens(F), drift(O), defocusing lens(D), and another drift(O). To see how this particular beam line affects the motion of the particle, we have to multiply each component's respective matrix to the particles position in the order at which the particle reaches that component. For this particular beam line, the matrix representation is

$$\begin{bmatrix} \hat{x} \\ \hat{x'} \end{bmatrix} = \begin{bmatrix} 1 & L \\ 0 & 1 \end{bmatrix} \begin{bmatrix} 1 & 0 \\ \frac{1}{f} & 1 \end{bmatrix} \begin{bmatrix} 1 & L \\ 0 & 1 \end{bmatrix} \begin{bmatrix} 1 & 0 \\ -\frac{1}{f} & 1 \end{bmatrix} \begin{bmatrix} x \\ x' \end{bmatrix}$$

This is an effective way of quickly computing the position of a particle as it travels along its path. One of the key advantages of calculating position this way is the ability to track the particle's position at each lens and after each drift. An example of tracing a particle in this method is shown in Figure 2.

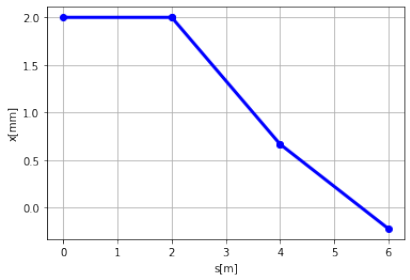

Figure 2: Example of a particle traveling through a FODO Lattice

However, this method can be quite cumbersome when simulating thousands of particles at once. There is a method of multiplying each particle by a single matrix instead of four matrices. Though, this does come at the cost of not knowing the particles positions between the start and finish of the beam line. This particular method requires that each beam line component matrix be multiplied together. The product of this multiplication is called the "equivalent element". By using it, the previous equation can be reduced down to

$$\begin{bmatrix} \hat{x} \\ \hat{x'} \end{bmatrix} = \begin{bmatrix} -\frac{L^2}{f^2} - \frac{L}{f} + 1 & \frac{L(L+2f)}{f} \\ -\frac{L}{f^2} & \frac{L}{f} + 1 \end{bmatrix} \begin{bmatrix} x \\ x' \end{bmatrix}$$

This method of particle tracing will be used in the next section.

2.3 Expanding to 3D

The final step before I was able to analyze various beam line arrangements was to expand the matrices to suit for both the x and y directions. Below are the updated matrices.

Lens

$$\begin{bmatrix} \hat{x} \\ \hat{x'} \\ \hat{y} \\ \hat{y'} \end{bmatrix} = \begin{bmatrix} 1 & 0 & 0 & 0 \\ -\frac{1}{f} & 1 & 0 & 0 \\ 0 & 0 & 1 & 0 \\ 0 & 0 & \frac{1}{f} & 1 \end{bmatrix} \begin{bmatrix} x \\ x' \\ y \\ y' \end{bmatrix}$$

Drift

$$\begin{bmatrix} \hat{x} \\ \hat{x'} \\ \hat{y} \\ \hat{y'} \end{bmatrix} = \begin{bmatrix} 1 & L & 0 & 0 \\ 0 & 1 & 0 & 0 \\ 0 & 0 & 1 & L \\ 0 & 0 & 0 & 1 \end{bmatrix} \begin{bmatrix} x \\ x' \\ y \\ y' \end{bmatrix}$$

There are two important features in these matrices. The first is the x and y positions are independent. The second is when a lens focuses a particle in one

direction, it defocuses it in the other direction. This is a problematic hurdle that is explored in later sections.

Using these matrices allows for 3D plots of particles traveling through the beam line. An example of a particle traveling in 3D is in Figure 3.

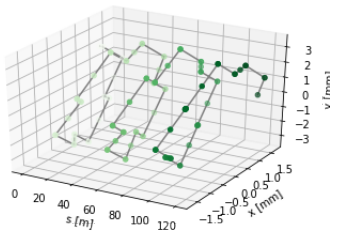

Figure 3: A particle traveling through a beam line in 3D

3 FODO Lattices

3.1 Testing FODOs

One of the more applicable lens arrangements is known as a FODO Lattice. As previously mentioned, a FODO Lattice consists of two lenses, one focusing and the other defocusing, separated by some drift distance. One of the issues that a FODO Lattice attempts to mitigate is the focusing asymmetry between the x and y directions. The FODO lattice focuses the particle in one direction and defocuses it in the other direction, allows for the particle to move down the beam line, then reaches a lens that will defocus the particle in the direction it was originally focused and focus the particle in the direction it was originally defocused. In an ideal situation, the FODO cell should be able to prevent any particle from going out of control and spiraling away from the optical axis.

Unfortunately, this ideal situation is difficult to achieve. I spent several days trying different FODO lattices to see if any were able to sufficiently stabilize the beam. I found that it was nearly impossible to blindly find a FODO arrangement that could stabilize particles in both directions.

When checking for beam stability, I was checking before and after distribution graphs. These graphs showed the spatial distribution of particles before and after the beam line. The key data I was looking for was the mean position and the standard deviation in each direction. Figure 4 is an example of one of these graphs. From Figure 4, it is clear to see that the spread of the distribution had increased in both the x and y directions. I seldomly found FODO lattices that were able to stabilize particles in one direction. And when I did, they almost always were unstable in the other direction. Eventually, I stumbled across an interesting result.

I found that putting two FODO lattices consecutively could produce a desirable result given the proper parameters. Figure 5 showcases the distribution graphs of two consecutive FODO cells with the parameter $f = \sqrt{L}$.

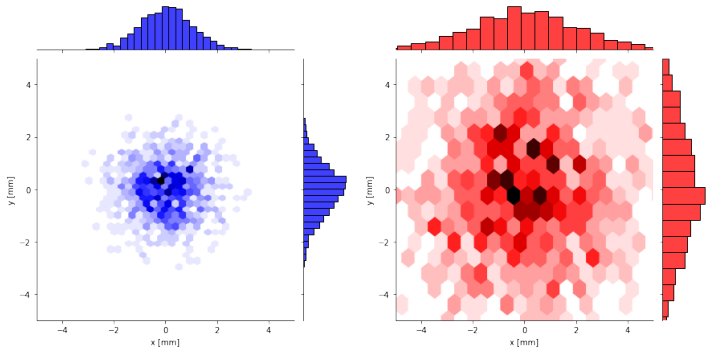

Figure 4: Distribution of 1000 particles before and after beam line

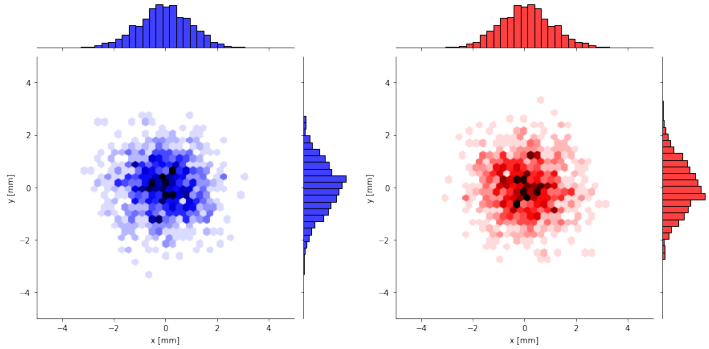

Figure 5: Distribution of 1000 particles before and after two FODO Lattices

The first feature that surprised me was that the standard deviations in both directions had not changed by any amount. They had remained constant even though the particles had traveled 8 meters. Secondly, I observed that the final distribution was geometrically an 180° rotation of the initial distribution. I then postulated and proved that having four of these particular FODO lattices generated a final distribution that was identical to the original after traveling 16 meters. Figure 6 shows a plot of 10 particles traveling through this particular lens system.

The 3D plot in Figure 6 showcases this strange behavior. The answer to why this behavior occurs lies in the equivalent matrix for this arrangement. When $f = \frac{L}{-\sqrt{2}}$, the equivalent matrix becomes

$$\begin{bmatrix} 1 & 0 & 0 & 0 \\ 0 & 1 & 0 & 0 \\ 0 & 0 & 1 & 0 \\ 0 & 0 & 0 & 1 \end{bmatrix}$$

Discovering this particular lens arrangement had an equivalent matrix that is the

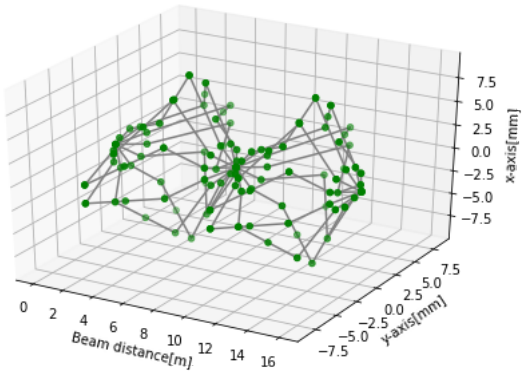

Figure 6: 10 particles traveling through two sets of double FODO lattices

identity matrix was quite surprising. It explained why the distribution hadn't changed after the particles exited the beam line. This result shows that FODO lattices could potentially be an arrangement suitable for the $\pi E5$ experiment. It also proved that it is possible for a magnetic lens arrangement to have a net-zero affect on particles as they travel down a beam line. This idea is something to keep in mind when researching other arrangements.

3.2 Rear Principal Plane

In optics, a pairing of two lenses is said to have an effective focal length. The effective focal length is a measurement that depends on the focal lengths of the two lenses and their separation. By using the effective focal length, a system of two or more lenses can be reduced to a single lens. This principle also applies to beam line optics. Two magnetic lenses can be condensed to a single magnetic lens with an effective focal length that's dependent on the individual focal lengths of each constituent lens. Figure 7 is an example of how to find the effective lens location graphically.

As mentioned, the two lens system has an effective focal length. This effective focal length is measured with respect to the Rear Principle Plane. The Rear Principle Plane is located at the intersection of the initial and final ray. The plane is indicated by the cyan dashed line in Figure 7. Another method of finding the location of the Rear Principle Plane without ray tracing is by using the following equation

$$d = \frac{Lf_{eff}}{f_1}$$

with d being the distance away from the final lens, f_{eff} being the effective focal length, and f_1 being the focal length of the first lens. Figure 8 showcases two plots from a FODO lattice with equal and opposite focal lengths. The first displays how d varies as the separation distance increases. The second shows

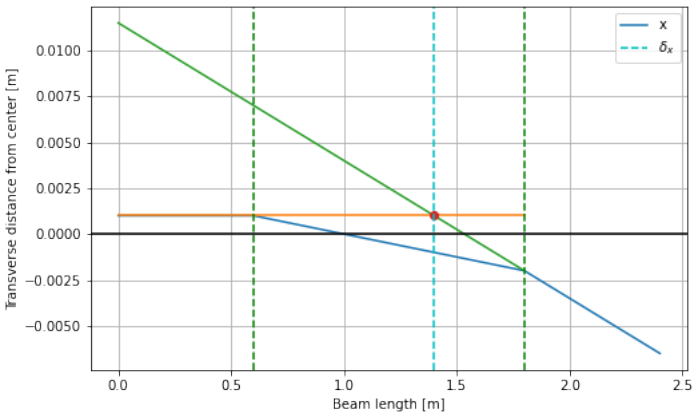

Figure 7: Example of ray tracing to find effective lens location (red dot)

how the effective focal length of the system changes as the separation distance increases.

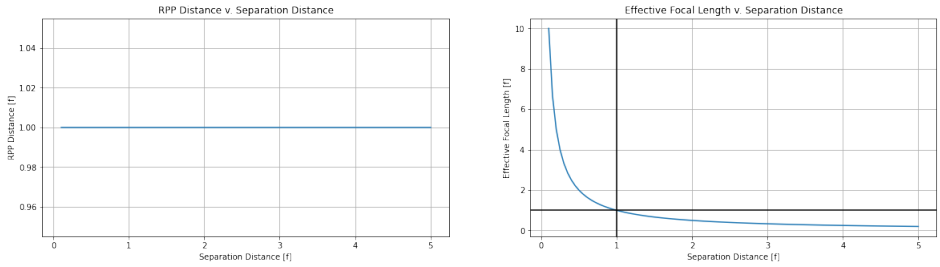

Figure 8: Testing the effect of separation distance on various parameters

The first graph in Figure 8 shows that the position of the RPP is independent of separation distance for double lens systems where the focal lengths are equal and opposite. The second graph in Figure 8 shows $d \propto \frac{1}{L}$. One specific feature to highlight is the effective focal length of the system is equal to the focal length of the first lens whenever the separation distance is also one focal length. This occurs because the particle hits the first lens and focuses towards the optical axis. Because the separation distance is the focal length, the particle will reach the second lens while on the optical axis . This causes the second lens to have no effect on the particle. Therefore, the effective focal length is simply the focal length of the first lens.

Studying the Rear Principle Plane location can be beneficial when constructing physical beam lines. Reducing a multiple lens system to a single lens can greatly reduce operation costs. It would also reduce error in computation due to less interactions. Understanding the effect of separation distance on the Rear Principle Plane location and effective focal length of a two lens system is also

important to know when viewing similar effects for three lens systems. These comparisons are explored further in a later section.

3.3 Astigmatism

Another phenomena in optics is known as an astigmatism. An astigmatism occurs when the focal lengths of a lens in perpendicular directions do not equal. For the particle application, this would be the focal lengths of a magnetic lens in the x and y directions. An example of a particle astigmatism is shown in Figure 9.

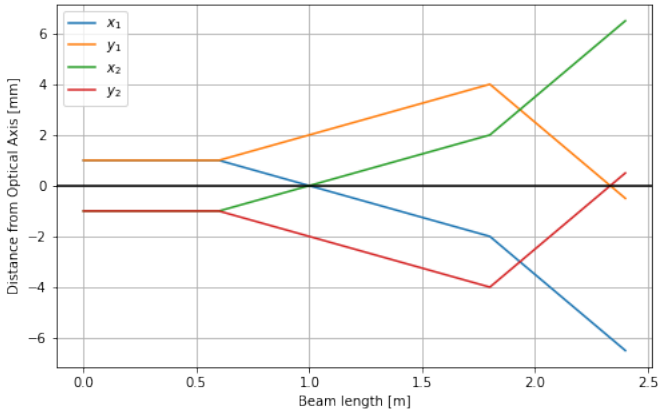

Figure 9: Particle Astigmatism

Figure 9 is a graph of two identical particles that were released from opposite ends of the transverse plane. The x coordinates of the two particles are colored blue and green while the y coordinates are colored orange and red. The astigmatism is apparent by noting the difference in position along the beam line at which the x coordinates intersect the optical axis and at which the y coordinates intersect the optical axis.

The ideal lens system would not have any evidence of an astigmatism at all. However, since each magnetic lens focuses in one direction and defocuses the other, it is nearly impossible to remove the astigmatism. I am currently looking into methods of reducing these astigmatisms. Astigmatisms of three lens systems are explored in a later section.

4 Triplets

4.1 Testing Triplets

Another arrangement of lens elements that are of research interest are triplets. Triplets are created by arranging three consecutive magnetic lenses. Typically,

the first and third lenses will have equivalent focal lengths while the middle lens will have a focal length of opposite parity. Figure 10 shows an example of a particle traveling through a triplet.

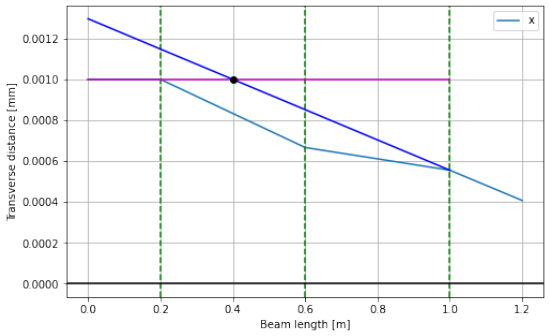

Figure 10: A single particle traveling through a triplet

Adding a third lens to this system introduces two more parameters: an extra separation distance and another focal length. As expected, the extra parameters make the analysis of a system's equivalent matrix a bit more difficult, but it also brings new opportunities in areas where FODO lattices fell short.

It should be noted that the triplet cells that were researched here had a special condition. The focal length of the first and third quadrupole were set equal to each other. This focal length is known as the "prime focal length". The focal length of the middle quadrupole was set to be a negative half of the prime focal length. This focal length is known as the "secondary focal length". Additionally, the separation distance between the first and second lens and the distance between the second and third lens are set equal to one another. All triplet cells mentioned are subject to these conditions.

4.2 Rear Principle Plane in Triplets

Similar to FODO cells, a rear principle plane exists for triplets. Figure 10 exemplifies the method of ray tracing used for FODO cells to find the location of the Rear Principle Plane. Additionally, a formula to find the distance from the third lens to the Rear Principle Plane can be constructed.

$$d = \frac{(d_{12}+L_2)f_{123}}{f_{12}}$$

Many new variables are introduced here. L_2 is the separation distance from the second to third lens. f_{123} is the effective focal length of the triplet system. f_{12} is the effective focal length of the lens system containing only the first and second lens. Finally, d_{12} is the distance from the second lens to the position of the Rear Principle Plane of the first and second lens system.

As convoluted as it sounds, this function can be graphed to show how the Rear Principle Plane distance varies as the separation distance is varied. The function is graphed in Figure 11.

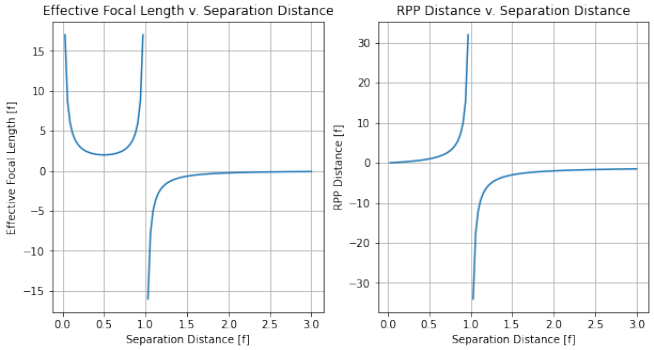

Figure 11: Graphing lens system parameters versus separation distance

The graphs in Figure 11 provide a greater intuition of how separation distance affects the two different system parameters. Specifically, the discontinuity at $L = f$ shows that the system doesn't seem to have much of an affect on incoming particles since the focal length and Rear Principle Plane distance approach infinity. Further interpretation of varying system parameters are still be studied.

4.3 Astigmatism in Triplets

One of the final topics I've reached as part of my research is analyzing astigmatisms in triplets. Astigmatisms are present in triplets just as they were in FODO cells. An example of astigmatism in triplets can be found in Figure 12.

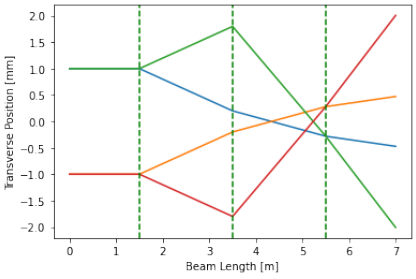

Figure 12: Example of astigmatism present in triplet lens system

Again, the astigmatism affects how particles can be focused to a single point on the optical axis. However, by reducing the separation distances and having the middle lens be half the focal length as the others, an astigmatism could potentially be avoided. Figure 13 showcases this system.

The lens arrangement displayed in Figure 13 doesn't necessarily avoid an astigmatism, but it does delay it. The exiting particles are bent slightly toward

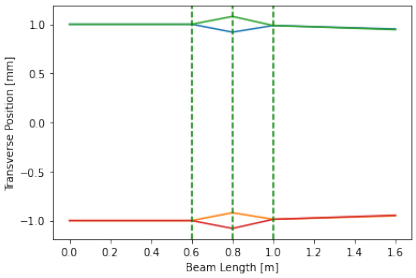

Figure 13: Particles passing through triplet with shortened separation

the optical axis and eventually cross and form an astigmatism. However, that occurs nearly 20 meters down the beam line. This particular triplet arrangement shows that particles may be able to be stabilized and kept from diverging too far from the optical axis before striking a target.

One idea that came up was to set the Rear Principle Plane distance in the x and y directions of a triplet cell equal to each other. Consequently, the result of setting the two variables together would give a relationship between the prime focal length and separation distance that results in the two RPPs becoming equivalent. Further, if the effective focal length in the x and y directions were equal while the triplet cell met the RPP condition, then, theoretically, the triplet cell would effectively bend the particle at the same point and the same amount in both the x and y directions resulting in no astigmatism.

Unfortunately, when solving for equivalent RPPs, the resulting sole condition is for $L = 0$. This shows that the RPP distance cannot be equivalent for both the x and y directions in a single triplet cell. However, it may be possible to set both RPP distances equal in a chain of two or more triplet cells.

4.4 Triplet Stability Condition

Some beamlines require repeated lattices to control particles. For example, circular storage rings can have particles travel through the same FODO and triplet cells billions of times. The stability condition can be used to ensure the beam remains stable as particles travel through the beamline. The stability condition can be derived from the sympletic property of the transfer matrices [3]. The stability condition for an arrangement of elements is

$$|Tr(M)| \leq 2$$

where M is the equivalent matrix.

Given the equivalence matrix of a triplet with a , its trace can be calculated. The trace is $2 - \frac{4L^2}{f^2}$. Consequently, the triplet stability condition becomes

$$0 \leq \frac{L}{f} \leq 1$$

Therefore, in order for a beamline to remain stable inside of a triplet cell, the separation distance must not be longer than the prime focal length. Figure 14 is a graph comparing particle behavior in stable and unstable triplet cells.

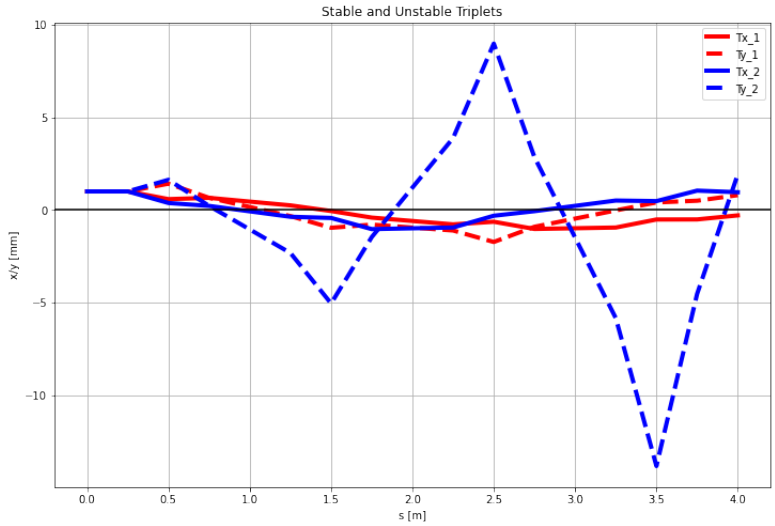

Figure 14: Graphing identical particle through 5 stable and unstable triplet cells

As Figure 14 shows, the stable triplet cell (red) produces a particle path that remains within about 2mm from the optical axis in either direction. Whereas, the unstable triplet cell (blue) produces unstable motion in the y direction.

5 Additional Findings

5.1 One Meter Restriction

An interesting idea that Dr. Gorringe had given me was to investigate how effective a single FODO cell is at focusing a particle compared to how effective a triplet cell is at focusing a particle given two constraints: both cells must span one meter and both must have equivalent effective focal lengths. As previously mentioned, the effective focal lengths in both transverse directions can never be equal. So, I ran two trials, one for each of the transverse directions. Figure 15 and 16 showcase the results from exploring this idea.

In both cases, the triplet cell was more effective at focusing the particle over the meter. The position of the particle traveling through the triplet cell became close to the optical axis in both transverse directions. Conversely, the position of the particle traveling through the FODO cell only reached closer to the optical axis in the x direction. This could be useful to know in cases where a single cell is needed in a beamline.

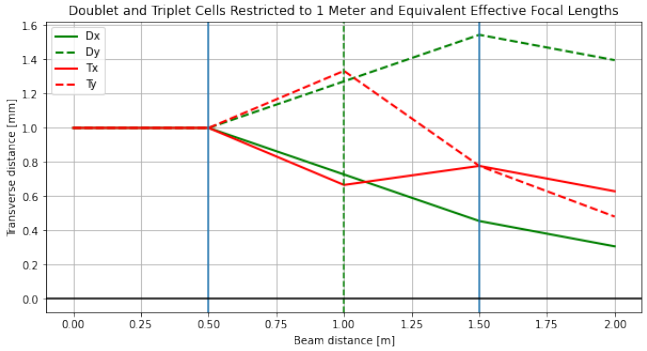

Figure 15: Single meter restriction with equivalent effective focal length in x direction

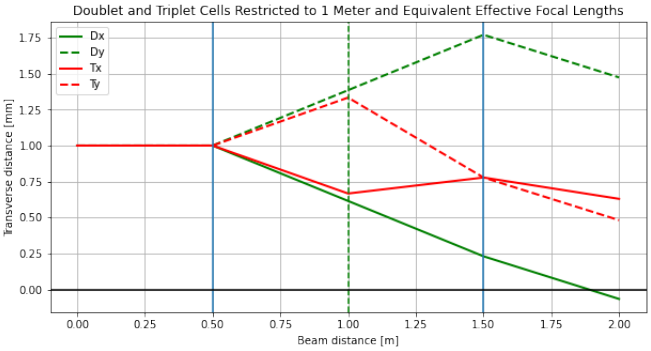

Figure 16: Single meter restriction with equivalent effective focal length in y direction

5.2 Dipole Implementation

Another common component found in beamlines is the dipole. The role the dipole plays in particle beamlines is to bend particles in the longitudinal direction. The transfer matrix for the dipole is

$$\begin{bmatrix} cos(\frac{l}{\rho}) & \rho sin(\frac{l}{\rho}) & 0 & 0 \\ -\frac{1}{\rho}sin(\frac{l}{\rho}) & cos(\frac{l}{\rho}) & 0 & 0 \\ 0 & 0 & 1 & l \\ 0 & 0 & 0 & 1 \end{bmatrix}$$

A few new parameters have been introduced here. The parameter ρ represents the bending radius of the beamline. The parameter l is the arclength of the path traveled. The importance of the dipole isn't so clear in the current state of the simulation. The real beauty of the dipole comes when momentum is taken into account. Then, the dipole can be used to filter out unwanted par-

ticles from the beamline. Unfortunately, there wasn't quite enough time to fully implement momentum into the simulation. Momentum implementation can get fairly convoluted when compared to the current simulation. The next major step for the simulation is to implement momentum.

6 Conclusion

At the end of the summer, I believe I have used the particle beamline simulation to show some interesting properties of beamlines. Although the simulation is far from including every conceivable element and transfer matrix, it does supply a basic understanding of how beamline elements work and how they will affect particle motion. At the bare minimum, I hope that Dr. Gorringe and his fellow researchers will find the simulation beneficial as they begin working with the $\pi E5$ beamline at the Paul Scherrer Institute.

7 Acknowledgments

I would like to thank the University of Kentucky Summer Undergraduate Research Fellowship for funding this project. I would also like to thank Dr. Chris Crawford for allowing me to be a participant in the University of Kentucky REU program. Finally, I would like to thank Dr. Tim Gorringe for his great insight towards this project and his dedication to support me in this endeavor.

References

[1] PIONEER Collaboration, W. Altmannshofer, H. Binney, E. Blucher, D. Bryman, L. Caminada, S. Chen, V. Cirigliano, S. Corrodi, A. Crivellin, S. Cuen-Rochin, A. Di Canto, L. Doria, A. Gaponenko, A. Garcia, L. Gibbons, C. Glaser, M. Escobar Godoy, D. Göldi, S. Gori, T. Gorringe, D. Hertzog, Z. Hodge, M. Hoferichter, S. Ito, T. Iwamoto, P. Kammel, B. Kiburg, K. Labe, J. LaBounty, U. Langenegger, C. Malbrunot, S. M. Mazza, S. Mihara, R. Mischke, T. Mori, J. Mott, T. Numao, W. Ootani, J. Ott, K. Pachal, C. Polly, D. Počanić, X. Qian, D. Ries, R. Roehnelt, B. Schumm, P. Schwendimann, A. Seiden, A. Sher, R. Shrock, A. Soter, T. Sullivan, M. Tarka, V. Tischenko, A. Tricoli, B. Velghe, V. Wong, E. Worcester, M. Worcester, and C. Zhang. Testing lepton flavor universality and ckm unitarity with rare pion decays in the pioneer experiment, 2022.

[2] Wolfgang Hillert. Transverse linear beam dynamics, 2021.

[3] Hao Research Group of Accelerator Physics. Transverse dynamics, 2021.